https://dx.doi.org/10.1016/j.jmst.2020.04.060

Fabrication of Multifunctional Polydopamine-Coated Gold Nanobones for PA/CT Imaging and Enhanced Synergistic Chemo-photothermal Therapy

Jingwei Xu,[a#] Xiaju Cheng,[b#] Fuxian Chen,[b] Weijie Li,[c] Xiaohui Xiao,[c] Puxiang Lai,[e] Guopeng Xu,[f] Li Xu,[f*] Yue Pan.[cd*]

[a] *Department of Cardiothoralic Surgery, Suzhou Municipal Hospital Institution, Suzhou, 215002, P.R. China.*
[b] *Jiangsu Key Laboratory of Infection and Immunity, Institutes of Biology and Medical Sciences, Soochow University, Suzhou 215123, P. R. China*
[c] *Guangdong Provincial Key Laboratory of Malignant Tumor Epigenetics and Gene Regulation, Medical Research Center, Sun Yat-Sen Memorial Hospital, Sun Yat-Sen University, Guangzhou 510120, P.R. China.*
[d] *Center for Precision Medicine, Sun Yat-Sen University, Guangzhou, 510080, P.R. China.*
[e] *The Hong Kong Polytechnic University, Department of Biomedical Engineering Kowloon, Hong Kong SAR, China.*
[f] *Department of Respiratory Medicine, Suzhou Municipal Hospital Institution, Suzhou, 215002, P.R. China.*
[#]*Equal contribution*
[*]*Corresponding author: xuli198008@126.com, panyue@mail.sysu.edu.cn*

Abstract: Multimodal imaging-guided chemo-photothermal therapy is an excellent cancer treatment, which can not only efficiently against tumor, but also can offer precise treatment window and real-time monitoring of the treatment efficiency. In our work, polydopamine (PDA)-coated gold nanobones (AuNBs@PDA nanocomplexes) were designed for this approach. The AuNBs@PDA nanocomplexes have strong absorbance in the near infrared (NIR) region and higher photothermal conversion efficiency (75.48%) than gold nanobones alone, which was facilitated for photoacoustic imaging and photothermal therapy. Besides, the loading efficiency of doxorubicin (DOX) by AuNBs@PDA nanocomplexes could be up to about 70% and DOX release from AuNBs@PDA/DOX nanocomplexes sensitively response to the lower pH environment and NIR laser irradiation, which makes them become the excellent nano-carrier for the delivery of chemotherapy drug. *In vitro* and *in vivo* studies showed significant cytotoxicity and antitumor efficacy by the AuNBs@PDA/DOX nanoplatform with negligible side effects. Meanwhile,

the nanoplatform was also successfully employed for computed tomography (CT) imaging, attributing to the high atomic number and high X-ray attenuation coefficient of gold. Therefore, we believed that the proposed PDA-coated gold nanobones would be a novel multifunctional theranostic nanoagent to realize the PA/CT imaging-guided chemo-photothermal therapy of cancer.

Keywords: Imaging, Photothermal therapy, Multifunctional nanobones

1. Introduction

In recent years, an increasing number of multifunctional diagnostic and therapeutic nanomaterial has been used for efficient and security antitumor therapy.[1, 2] Especially, the real-time imaging-guided photothermal therapy (PTT) is attracting more and more attention due to its noninvasiveness and safety.[3-5] PTT as an effective tumor therapy strategy is mediated by converting photon energy into heat to induce tumor cells death upon laser irradiation. In general, the PTT nanoagents can also be used for photoacoustic (PA) imaging by converting light energy into acoustic signals. In addition, the real-time PA imaging can monitor the process and efficiency of cancer treatment, when PTT nanoagents are accumulated at the tumor site, simultaneously enhancing the therapeutic efficiency.[6] Although the PTT alone is effective to inhibit tumor growth, it is difficult to completely eliminate the tumor due to the scattering of light in biological tissues. Therefore, scientists are interested in combination therapy that may have the stronger synergetic antitumor effect, such as chemo-photothermal therapy. As one of the major treatments for tumor, chemotherapy has poor selectivity and nonnegligible side effects. Thus, in a lot of chemo-photothermal therapy studies, PTT nanoagents have been used to enhance chemical drug targeting delivery as carriers.[7-10]

Inorganic gold nanomaterials have attracted a lot of attention and widely been used in biomedicine field because of their unique optical, electrical and chemical properties.[11-14] Different morphologies of gold nanomaterials have been applied to be computed tomography (CT) imaging contrast nanoagents, such as gold nanospheres,[15] gold nanorods,[16] and gold nanocages.[17] The gold element has not only

high X-ray attenuation coefficient (Z = 79, K-edge value = 80.73 keV), but also superior biological inert and biocompatibility.[18] Recently, various gold-based multifunctional nanomaterials raise concern and have been designed for tumor therapy, such as Au@Fe_3O_4,[19] Au@graphene oxide,[20] Au@MnO_2[21] and Au@CuS.[22] These nanomaterials have not only the function of their components, but also the synergistic effect, whose prospective biomedical application is more anticipated.[23-25] Since it was reported that the mussel-inspired adhesive protein can be applied for multifunctional coating by Messersmith et al in 2007,[26] polydopamine (PDA) has attracted substantial interests owing to its good properties of biocompatibility and easy surface modification.[27-30] According to the latest reports, due to its strong NIR absorption and high drug loading efficiency, PDA can be used as a universal surface coating of functional nanomaterial,[31, 32] including the gold nanomaterials. The published examples of PDA-coated gold nanomaterials were roughly divided into the following two types: (1) PDA-coated gold nanoparticles. Li et al. reported Au@PDA@BD nanoparticles for CT imaging and PTT.[33] Sun et al. reported Au@PDA-125I particles for SPECT/CT imaging and radiosensitization.[34] (2) PDA-coated gold nanorods, Liu et al. reported AuNR@CuPDA for PPT and chemotherapy.[35] Khlebtsov et al. reported AuNR-PDA-R123-folate nanoparticles for targeted fluorescent imaging and PTT.[36] Wang et al. reported AuNR-PDA MB/DOX for PTT combined photodynamic or chemotherapy.[37] Besides, there are some other nanostructures, such as PDA-coated gold nanostars,[38] and PDA-coated branched Au-Ag nanoparticles.[39] In a word, these nanomaterials are competitive candidates in multimodal theranostic applications.

In this work, we fabricated a multifunctional platform from a PDA-coated gold nanobones (AuNBs) loaded with a chemotherapy drug, doxorubicin (DOX) (referred as AuNBs@PDA/DOX nanocomplexes), and simultaneously explore the potential applications in clinics. As shown in Scheme 1, the AuNBs@PDA/DOX nanocomplexes were designed by *in situ* polymerization of dopamine onto the surface of gold nanobones, then the DOX was loaded through π-π stacking and hydrogen binding interactions with PDA. The obtained AuNBs@PDA/DOX nanocomplexes exhibit strong absorbance in

the near-infrared (NIR) region, excellent photothermal conversion efficiency, and high drug loading capability. Upon laser irradiation, the AuNBs@PDA/DOX nanocomplexes could produce heat and increase DOX release, realizing the synergetic chemo-photothermal therapy. In addition, Au acted as CT contrast agent[15] and PDA could be used for PA imaging, respectively.[8] Therefore, the AuNBs@PDA/DOX nanocomplexes were employed as nanotheranostic agents for multimodal imaging-guided (PA/CT) imaging-guided synergetic chemo-photothermal therapy of cancer.

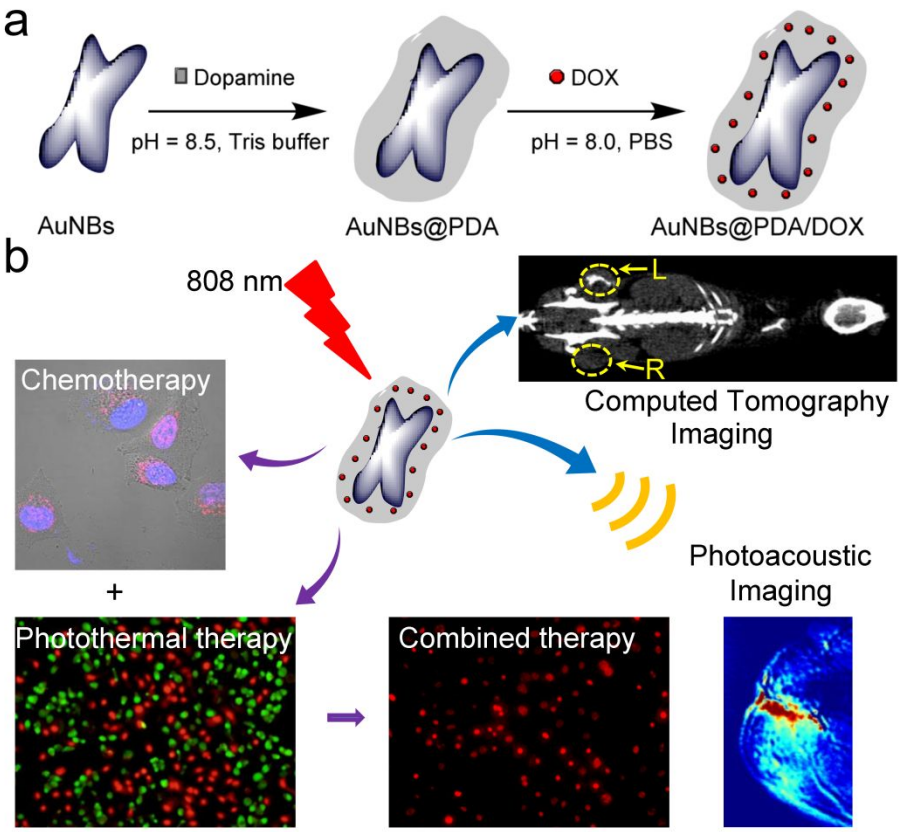

Scheme 1. (a) The diagram of the AuNBs@PDA/DOX nanocomplexes preparation; (b) The AuNBs@PDA/DOX nanocomplexes used for PA/CT imaging-guided chemo-photothermal therapy of cancer.

2. Experimental Section

2.1 Materials

Chloroauric acid ($HAuCl_4 \cdot 3H_2O$), hexadecyltrimethylammonium chloride (99%, CTAC), ascorbic acid (99.7%, AA) and sodium borohydride (98%, $NaBH_4$), silver nitrate (99.8%, $AgNO_3$), methyl thiazolyl tetrazolium (MTT), Doxorubicin hydrochloride (DOX) were purchased from Sigma Aldrich. Dopamine bought from Alfa Aesar. Live/dead cell staining kit (calcein-AM-propidium iodide) from Invitrogen. All chemicals were analytical grade and without further purification. Water used in the experiment was purified by a Milli-Q Water Purification System.

UV-vis-NIR absorption spectra were examined with UV spectrometer (UV-3600, Shimadzu). The instrument of dynamic light scattering (DLS) was Nano ZS90 form Malvern. Transmission electron microscopy (TEM) (Tecnai G2 Spirit, FEI) was used to display the morphology of particles. The 808 nm laser was MDL-N-808-10 W (Changchun New Industries Co., Ltd). The fluorescence imaging was performed on an Olympus fluorescent microscope (Tokyo, Japan).

2.2 Synthesis of PDA-coated gold nanobones

The AuNBs with diameter approximately of 50 nm length and 20 nm wide，which were synthesized following seed-mediated growth method. Gold nanoseeds were first synthesized as follows, CTAC (hexadecyltrimethylammonium chloride, 0.1 M, 10 mL) and $HAuCl_4$ (10 mM, 250 μL) were stirred for 5 min, then 0.6 mL of 10 mM $NaBH_4$ was added when the solution colour from yellow into brown. Next, the AuNBs growth solution was prepared by dissolving CTAC (0.1 M, 10 mL), $AgNO_3$ (3 mM, 100 μL), HCl (1 M, 200 μL) and $HAuCl_4$ (10 mM, 0.5 mL) in a 50 mL Erlenmeyer flask. The mixture let to stand at 30 °C for 15 min, then added 0.1 mL of 100 mM ascorbic acid and vigorously stirred for 30 s. At last, the mixture solution was added 10 μL gold nanoseeds solution. Vigorously stirring for 30 s, the mixture let to stand at 30 °C for 12 h for AuNBs growth. After synthesis, surfactant was removed by centrifugation and washing with PBS for two times. The resulting AuNBs solution was preserved at 4 °C for further experiments. The PDA coating was prepared according to the technique described by the previous reports.[26] 1 mg of AuNBs was added to the dopamine solution (2 mM, 1 mL), and adjusted pH to 8.5 using tris (hydroxymethyl) aminomethane buffer. Then the solution was sonicated for 20 min

for PDA coating. The AuNBs@PDA nanocomplexes were obtained by centrifugation. And at last, the PEG-modified AuNBs@PDA nanocomplexes were obtained by covalently functionalized with amine-terminated PEG (mPEG-NH_2, 5 kDa).

2.3 DOX loading and release

For DOX loading, different concentrations of DOX (0, 25, 50, 100, 150, 200, and 250 μg/mL) were added to the 1 mg/mL AuNBs@PDA nanocomplexes solution. The mixture was agitated at 25 °C for 6 h. And the mixture was centrifugated with deionized water three times to remove the redundant DOX. The obtained DOX loaded nanocomplexes (AuNBs@PDA/DOX) were re-suspended in deionized water and preserved at 4 °C for next experiments. The loading efficacy of DOX was calculated by UV-vis-NIR absorbance. For DOX release, AuNBs@PDA/DOX nanocomplexes were dialyzed in PBS buffer of pH 7.2 and 6. And the temperature of buffer was almost 37 °C. At 0, 0.25, 0.5, 1, 3, 5, 7, 9, 11, and 24 h time points, the relieving DOX from AuNBs@PDA/DOX nanocomplexes was collected and calculated. Besides, at the different time points, the AuNBs@PDA/DOX nanocomplexes in pH 6 solution was irradiated with an NIR laser (808 nm, 1W/cm^2) for 5 min. Then, the release DOX was collected and calculated.

2.4 Calculation of photothermal conversion efficiency

To measure the photothermal conversion efficiency of the AuNBs@PDA nanocomplexes, different concentrations of AuNBs@PDA nanocomplexes (0, 12.5, 25, 50, and 100 μg/mL) were irradiated with the 808 nm laser (1 W/cm^2) for 5 min. And 50 μg/mL AuNBs@PDA nanocomplexes were also irradiated with the 808 nm laser at various power densities (0, 0.25, 0.5, 0.75 W/cm^2) for 5 min. The original temperature was maintained at 26 ± 2 °C. A digital thermo imaging was used to measure the real time temperature of the AuNBs@PDA nanocomplexes during irradiation, and the distilled water as a control. The photothermal conversion efficiency was calculated with the following equation according to a previously reported method.

$$\eta = \frac{mc(T_{max} - T_{max,\ H_2O})}{I(1 - 10^{-A})\tau_S}$$

where m is the solution mass, c is 4.2 J/g, the heat capacity of water, T_{max} and $T_{max,\ H2O}$ are maximum temperatures achieved in the presence or absence of the AuNBs@PDA, i.e., 67.5 °C and 28.0 °C, respectively, I is the power density of 808 nm laser (1 W/cm^2), A is the 808 nm absorbance of AuNBs@PDA solution (1.79), and τ_s is system time constant (223.35 s).

2.5 Cellular uptake of free DOX and AuNBs@PDA/DOX

Murine breast carcinoma cell line 4T1 cells were seeded into 35 mm dish at a density of 1×10^4 cells for 24 h, then incubated with 50 μg/mL AuNBs@PDA/DOX nanocomplexes (loading DOX, 6.6 μg/mL) and the same amount of free DOX for 2 h. After that, the cells were washed with PBS for three times and stained the nuclear with DAPI. At last the cellular uptake of free DOX and AuNBs@PDA/DOX were observed using the Olympus fluorescent microscope.

2.6 Chemo-photothermal therapy of tumor cells *in vitro*.

To investigate the chemo-photothermal combination therapy efficiency of AuNBs@PDA nanocomplexes, in brief, 4T1 cells were seeded into 96-well plates at a density of 5×10^3 cells/well for 24 h, and incubated with free DOX, AuNBs@PDA and AuNBs@PDA/DOX nanocomplexes at different concentrations for 24 h. Then the cells were exposed to the 808 nm laser (1 W/cm^2) for 5 min. After another 24 h, the relative cell viability of different treatment groups was measured by MTT cell proliferation cytotoxicity assay kit compared with untreated control group. And the chemo-photothermal synergetic therapy effect was further detected by live/dead staining analysis using fluorescence microscope. 4T1 cells were seeded in 12-well plate at a density of 5×10^4 cells per well. After incubating for 24 h, the cells were set to six groups (including control, free DOX, AuNBs@PDA, AuNBs@PDA/DOX, AuNBs@PDA + NIR, and AuNBs@PDA/DOX + NIR groups. NIR = 808 nm laser, 1 W/cm^2, 5 min, C_{DOX} = 6.6 μg/mL, $C_{AuNBs@PDA}$ = 50 μg/mL) and treated as mentioned above MTT

assay. After treated, then the cells were stained with live/dead cell staining kit (Invitrogen) for 30 min and observed using confocal microscope. The live cells were green and dead ones were red.

2.7 Tumor Model

BALB/c mice were achieved from Changzhou cavens laboratory animal technology Co. Ltd. and used under the protocol approved by Soochow University laboratory animal center. We subcutaneously injected 1×10^6 4T1 cells at the back of mouse. All procedures used in this experiment were compliant with the animal ethics committee of Soochow University Laboratory Animal Center.

2.8 PA/CT imaging

A small animal imaging system MSOT (iThera Medical, Germany) was used for *in vitro* and *in vivo* PA imaging. Different concentrations of AuNBs@PDA nanocomplexes (0, 6.25, 12.5, 25, 50, and 100 μg/mL) were planned to evaluate *in vitro* testing. For *in vivo* testing, 100 μL, 2 mg/mL AuNBs@PDA nanocomplexes were injected into the 4T1 tumor-bearing mice via tail vein. After different time points (0, 0.5, 1, 3, 6, 9, and 12 h), the mice were anesthetized and placed into the MOST measurement. The PA signal of tumor was collected immediately.

For CT imaging, different concentrations of AuNBs@PDA nanocomplexes (0, 62.5, 125, 250, 500, and 1000 μg/mL) were prepared in 1 mL centrifuge tubes. The same concentrations of iopromide were used as control. For *in vivo* CT imaging, the mice with tumors on both sides of the thigh were anesthetized. Then 100 μL AuNBs@PDA nanocomplexes (2 mg/mL) and the same amount of iopromide were intratumorally injected into the left and right side of the tumor, respectively. The CT images were scanned and acquired with a U-SPECT + /CT (MILabs) scanner.

***2.9 In vivo* chemo-photothermal therapy with the aid of AuNBs@PDA/DOX nanocomplexes**

For *in vivo* chemo-photothermal therapy of cancer, we firstly detected the photothermal properties of AuNBs@PDA nanocomplexes *in vivo*. 100 μL, 2 mg/mL AuNBs@PDA nanocomplexes were injected

into 4T1 tumor-bearing mice via tail vein, PBS as control. After 3 h, mice were irradiated with 808 nm laser (1 W/cm^2, 10 min) and recorded the tumor local temperature change with an infrared camera.

When the tumor on the back of mice reached approximately 75 mm^3, mice were stochasticly divided into four groups (including NIR, DOX + NIR, AuNBs@PDA + NIR, and AuNBs@PDA/DOX + NIR groups). In all groups, NIR was the group that the cells were irradiated with 808 nm laser (1 W/cm^2) for 10 min as control. Mice from the "DOX + NIR" group were injected with DOX at the 1.3 mg/kg body weight. The other groups of mice were injected with 100 μL, 2 mg/mL AuNBs@PDA or AuNBs@PDA/DOX (equivalent DOX 1.3 mg/kg body weight) via tail vein. After 3 h, the mice were anesthetized and irradiated with 808 nm laser (1 W/cm^2) for 10 min. In the meantime, the tumor growth was monitored by tumor size and weight every other day with a calliper and an electronic balance. And the tumor volume (V, mm^3) was calculated as follows: $V = (a \times b^2) / 2$, a (mm) is tumor length and b (mm) is tumor width, respectively. The tumor growth inhibition (TGIR) was calculated as follows: $TGIR = (1 - V/V_{NIR}) \times 100\%$. H&E staining of tumor from mice was performed on the 2nd day post treatment. And an inverted microscope was used to observe the staining.

3. Results and Discussion

3.1 Characterization of AuNBs@PDA nanocomplexes

To prepare the AuNBs@PDA nanocomplexes, AuNBs were fabricated by a classic seed-mediated growth procedure according to the previously reported method.[40, 41] Initiatlly, almost 5 nm size of gold nanoseeds were synthesized. Then gold nanobones were grown on the seeds by hexadecyltrimethylammonium chloride (CTAC) as template. The average size of obtained gold nanobones was length of 44.2 ± 1.4 nm and diameter of 18.7 ± 1.4 nm (Figure 1a). Then the CTAC was removed through centrifugation and we coated the AuNBs with PDA for further surface functional modification. The PDA coating was achieved by the amino ligand of dopamine binding to the gold surfaces and self-polymerization of dopamine under alkaline conditions as reported in the previous

paper.[16, 42] The TEM image of AuNBs@PDA nanocomplexes showed that PDA shell was approximately thickness of 8 nm (Figure 1b). And the hydrodynamic size and zeta potential of AuNBs and AuNBs@PDA nanocomplexes were measured by DLS. As shown in Figure S1a, the results showed that the CTAC capped AuNBs have two peaks of average hydrodynamic size 56.2 nm and 3.4 nm, and AuNBs@PDA nanocomplexes have only one peak of average hydrodynamic size 150.9 nm. The large hydrodynamic size of AuNBs@PDA nanocomplexes may be due to PEG modification on the surface. And the hydrodynamic size of AuNBs@PDA nanocomplexe was almost unchanged in PBS and 10% FBS DMEM medium within 48 h (Figure S1b). And as shown in Figure S1c, the zeta potential of CTAC capped AuNBs was 28.0 ± 1.6 mV. After we coated AuNBs with PDA, the zeta potential of AuNBs@PDA nanocomplexes was changed to -12.6 ± 2.5 mV. Moreover, the transverse and longitudinal local surface plasmon resonance (LSPR) peaks of AuNBs were approximately 552 nm and 667 nm detected by an UV-vis-NIR absorption spectra (Figure 1c). After coated with PDA, the absorption of AuNBs@PDA become broad and bathochromic shift especially increase absorption in the 700-1000 nm NIR.

The excellent NIR absorption of AuNBs@PDA nanocomplexes encouraged us to explore its photothermal property. Firstly, the photothermal properties of AuNBs@PDA nanocomplexes were investigated by supervising the rise of temperature upon the 808 nm laser irradiation. As shown in Figure 1d, the real-time temperature of AuNBs@PDA nanocomplexes aqueous solutions was gradually increased with the extension of irradiation time，and it is concentration of AuNBs@PDA nanocomplexes dependent. 5 min post irradiation, the temperature of the 50 μg/mL AuNBs@PDA nanocomplexes was raised from 26 °C to 60 °C. In contrast, the temperature of water increased only 2 °C in the same condition. And we also irradiated the 50 μg/mL AuNBs@PDA nanocomplexes with the 808 nm laser at various power densities. During continuous irradiation, the temperature of the solutions rapidly rose initially along with the irradiation power (Figure S2a). In addition, the photothermal stability was another vital factor of photothermal therapy agent. The temperature elevation of AuNBs@PDA nanocomplexes

were maintained upon laser irradiation for four on/off cycles (Figure S2b). Moreover, the photothermal conversion efficiency (η) of AuNBs@PDA nanocomplexes was up to 75.48 % calculated by a previous method (Figure S2c& Figure S2d).[22] Therefore, it is implied that the AuNBs@PDA nanocomplexes have the potential to be excellent nanoagents of photothermal therapy.

It was reported that DOX as an aromatic structure chemotherapy drug can be loaded on the surface of sp^2 – bonded polymers via π-π stacking and hydrogen binding, such as PDA.[43, 44] Therefore, we further studied the DOX loading efficiency of AuNBs@PDA nanocomplexes. For DOX loading, we first examined the absorption curves of DOX solutions with different concentrations using UV-vis-NIR absorption spectra. As shown in Figure S3a, the characteristic absorption region of DOX is about 500-600 nm, and the absorbance of peak was proportional to the concentration (Figure S3b). Then, 1 mg/mL AuNBs@PDA nanocomplexes were mingled with different amounts of DOX, shaking and reacting for 6 h in PBS (pH = 8). Post the reaction, DOX loaded AuNBs@PDA nanocomplexes were obtained after removing the unbound DOX via centrifugal filtration. The DOX loading efficiency (AuNBs@PDA: DOX, w/w) was calculated by detecting the supernatant excess DOX (Figure S3c). As shown in Figure 1e, the loading efficiency of AuNBs@PDA nanocomplexes was raised as the amount of DOX increase and it tended to be saturated. Concerned that loading plenty of DOX would affect the properties of nanoparticles, the feeding of 5:1 (AuNBs@PDA: DOX, w/w) was used for our followed experiments with DOX loading of 66%. Moreover, we also have investigated the drug release of the AuNBs@PDA/DOX nanocomplexes. Firstly, the AuNBs@PDA/DOX nanocomplexes suspended in different pH of PBS buffer were incubated and shaken for different time in 37 ^{o}C water bath. Then, we monitored the release amount of DOX (Figure S4) and calculated the percent of DOX release at various time points. As shown in Figure 1f, the results revealed that DOX have a favorable sustained release from the AuNBs@PDA/DOX nanocomplexes under more acidic conditions (pH = 6). After 24 h, the percent of DOX release were 17.4% at pH 7.2 and 43.9% at pH 6, respectively, which was consistent with the previous reports.[10, 16] At lower pH, the amino group of DOX molecule can be protonated, which speed

up the release of DOX from PDA nanoparticles.[45, 46] Moreover, we tested the DOX release from AuNBs@PDA/DOX nanocomplexes at pH values of 6 with NIR laser irradiation. Upon exposure of AuNBs@PDA/DOX nanocomplexes to NIR laser, the release of DOX was enormously increased. After 24 h, the percent of DOX release were up to 65.4%. And it confirmed that the effective photothermal heating property of AuNBs@PDA can be more conducive for DOX release, which may result in the destruction of intermolecular forces and hydrogen bonding.[8]

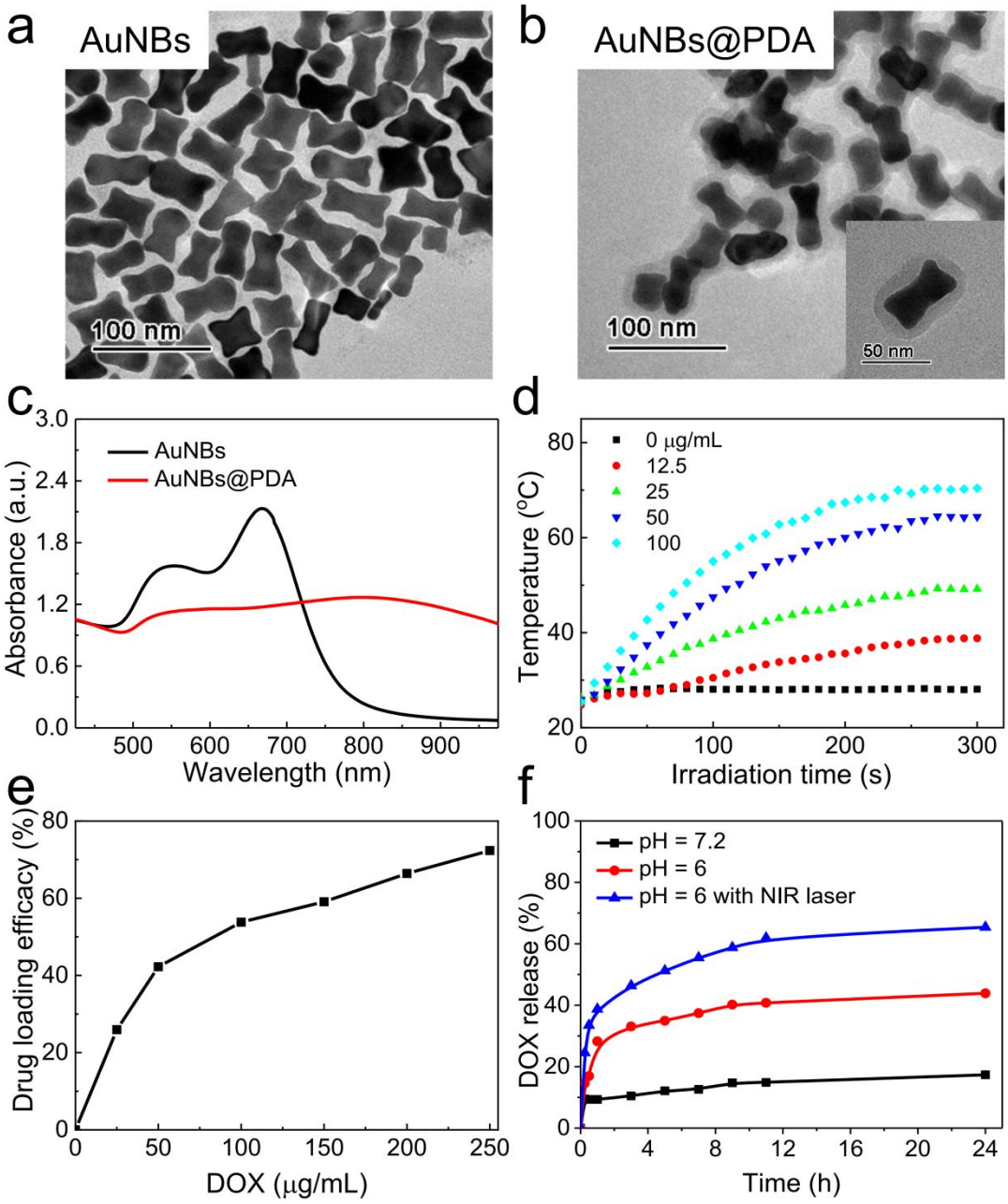

Figure 1. (a&b) TEM images of AuNBs and AuNBs@PDA; (c) Vis-NIR absorption spectra of AuNBs and AuNBs@PDA; (d) The photothermal heating curves of AuNBs@PDA nanocomplexes with different concentrations under 808 nm laser irradiation (1 W/cm^2) for 5 min; (e) Quantification of DOX loading at different feeding amounts of DOX; (f) DOX release from AuNBs@PDA/DOX nanocomplexes overtime in different pH values (7.2 and 6) buffers and DOX release from AuNBs@PDA/DOX nanocomplexes at pH values of 6 with NIR laser irradiation.

3.2 *In vitro* synergistic therapeutic efficacy of AuNBs@PDA/DOX nanocomplexes

For investigating the therapeutic efficacy of AuNBs@PDA/DOX nanocomplexes, we have detected their cellular uptake in the 4T1 cells through the confocal microscope. 4T1 cells were incubated with AuNBs@PDA/DOX nanocomplexes (loading DOX, 6.6 μg/mL) and the same amount of free DOX for 2 h. As shown in Figure S5, both free DOX and AuNBs@PDA/DOX nanocomplexes could be swallowed by 4T1 cells after 2 h incubation time. And it was no obvious difference in the cellular uptake of free DOX and AuNBs@PDA/DOX nanocomplexes within a short time.

Then, we also have detected the biocompatibility and photothermal ablation efficacy of AuNBs@PDA nanocomplexes *in vitro* using the MTT assays. As shown in Figure 2a, no obvious cytotoxicity of AuNBs@PDA nanocomplexes was observed in 4T1 cells even up to 50 μg/mL, predicting the great biocompatibility of the AuNBs@PDA nanocomplexes. However, the cell viability was obviously declined, when 4T1 cells were incubated with the same amount of AuNBs@PDA nanocomplexes following 808 nm laser irradiation (1 W/cm^2) for 5 min. It indicated that the AuNBs@PDA nanocomplexes could be excellent photothermal ablation nanoagent for cancer. In addition, we have investigated the cytotoxicity of AuNBs@PDA/DOX nanocomplexes and free DOX in 4T1 cells as well. As shown in Figure 2b, AuNBs@PDA/DOX nanocomplexes exhibited the similar cytotoxicity compared with free DOX at the same DOX quantity. It was mean that AuNBs@PDA/DOX nanocomplexes could also be used for chemotherapy for cancer.

More importantly, we investigated that whether AuNBs@PDA/DOX nanocomplexes could be well used in combination therapy of chemotherapy and photothermal therapy. As shown in Figure 2c, the cell viability of combination therapy was significantly reduced, superior to both single treatments. Especially, the cell viability was reduced to 8% when the concentration of DOX was 6.6 μg/mL. It was indicated that AuNBs@PDA/DOX nanocomplexes have the excellent synergistic chemo-photothermal therapy efficiency.

We further assessed the synergistic therapy efficiency of AuNBs@PDA/DOX nanocomplexes through live/dead cell staining experiments. 4T1 cells were stained with calcein AM (green fluorescence) and propidium iodide (PI, red fluorescence) to distinguish live cells and dead cells, respectively. As shown in Figure 2d, the cells treated with AuNBs@PDA nanocomplexes alone showed negligible cell death as well as the control group. In contrast, the AuNBs@PDA/DOX nanocomplexes plus laser irradiation group exhibited the highest cytotoxicity compared with other groups, which was in agreement with the MTT assay. These results demonstrated that AuNBs@PDA/DOX nanocomplexes showed an outstanding synergistic chemo-photothermal therapy effect on killing cancer *in vitro*.

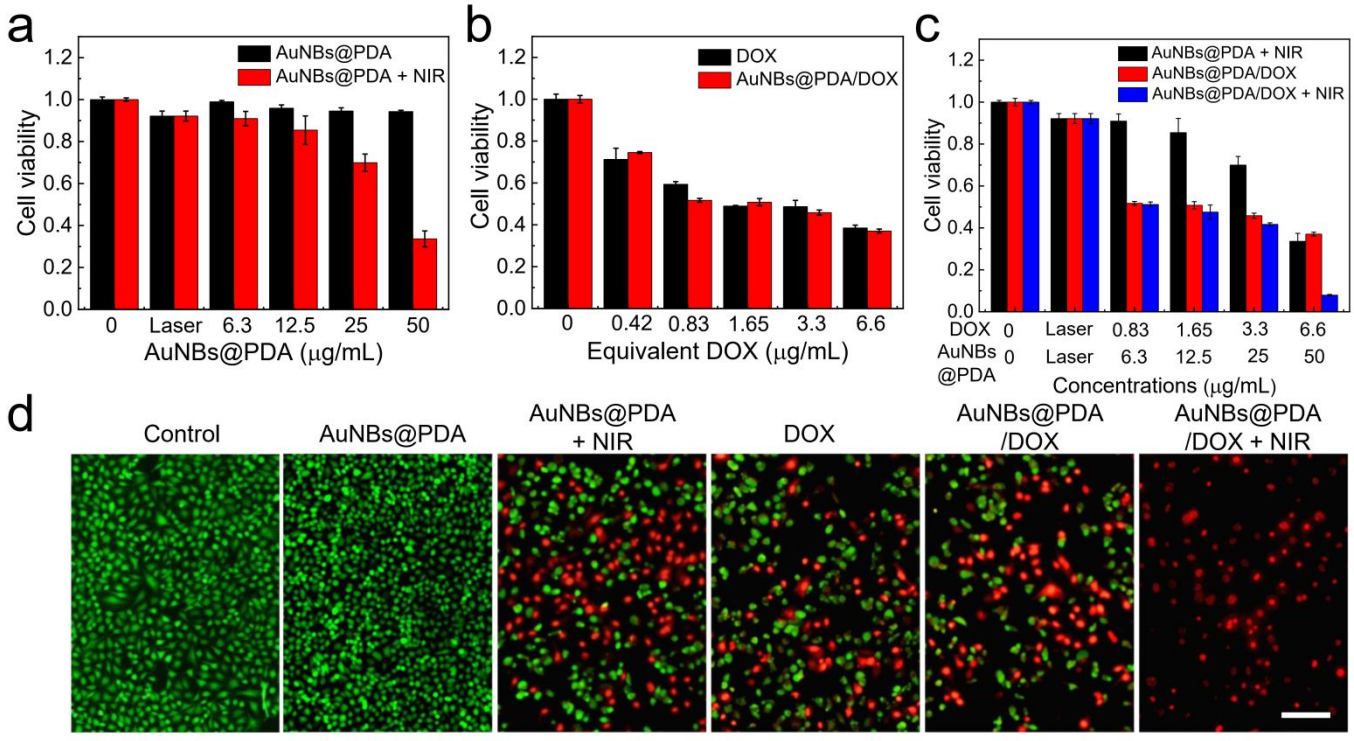

Figure 2. Chemo-photothermal therapy for cancer *in vitro*. (a&b&c) Cell viability of 4T1 cells after different treatments (NIR = 808 nm laser, 1 W/cm^2, 5 min, C_{DOX} = 6.6 μg/mL, $C_{AuNBs@PDA}$ = 50 μg/mL); (d) Live/dead fluorescence staining of 4T1 cells after different treatments. Scale bar = 50 μm.

3.3 Tumor imaging

The strong absorption of AuNBs@PDA nanocomplexes in the NIR motivated us to investigate its potential application as PA imaging contrast nanoagent. Because it have reported that NIR light can greatly enhance the penetration depth during the PA imaging of tumor.[47] Firstly, we have evaluated the PA signals of AuNBs@PDA nanocomplexes with different concentrations in aqueous solutions. As shown in Figure 3a, PA signals becomes obvious with the concentrations of AuNBs@PDA nanocomplexes increased and the intensity of PA signal is proportional to the concentrations (Figure S6). Moreover, the PA imaging capacity of AuNBs@PDA nanocomplexes was further tested *in vivo*. AuNBs@PDA nanocomplexes were injected into the tumor-bearing mice via tail vein and then the cross-sectional PA signal of tumor were obtained at different time points. As shown in Figure 3b, the PA image showed weak signal in the tumor at 0 h. But the signal was gradually enhanced post 0.5, 1, and 3 h injection. It could reach the maximum at 3 h and then the signal gradually decreased due to slowly metabolized out of the body of nanocomplexes. The PA signal of different time points at tumor site was also shown in the insert graph.

Besides, the atomic number and X-ray attenuation coefficient of gold nanomaterial is high, which triggered researchers focus on the CT imaging application of it.[48] To investigated the CT imaging capacity of AuNBs@PDA nanocomplexes, different concentrations of AuNBs@PDA nanocomplexes was firstly evaluated by phantom images *in vitro*. As shown in Figure S7a, the intensity of CT value (Hounsfield Unit, HU) becomes progressively stronger with the AuNBs@PDA nanocomplexes concentrations increased (Au concentrations: from 0 to 1 mg/mL). The CT value was calculated and shown in Figure S7b, a monotonic linear-increase with the concentration. Meanwhile, the CT value slope of AuNBs@PDA nanocomplexes was higher than iopromide, which was the commonly clinical CT

imaging agent. Then, the CT imaging function of AuNBs@PDA nanocomplexes was also evaluated *in vivo*. We transplanted 4T1 tumors to both sides of mouse. After 7 d, the mouse was anesthetized and injected with 100 μL AuNBs@PDA nanocomplexes (2 mg/mL) and equivalent iopromide in the left and right tumor, respectively. As shown in Figure 3c, the CT value of the left tumor site were observed much higher than the right. It was indicated that AuNBs@PDA nanocomplexes can be excellent CT imaging contrast nanoagent for cancer *in vivo*.

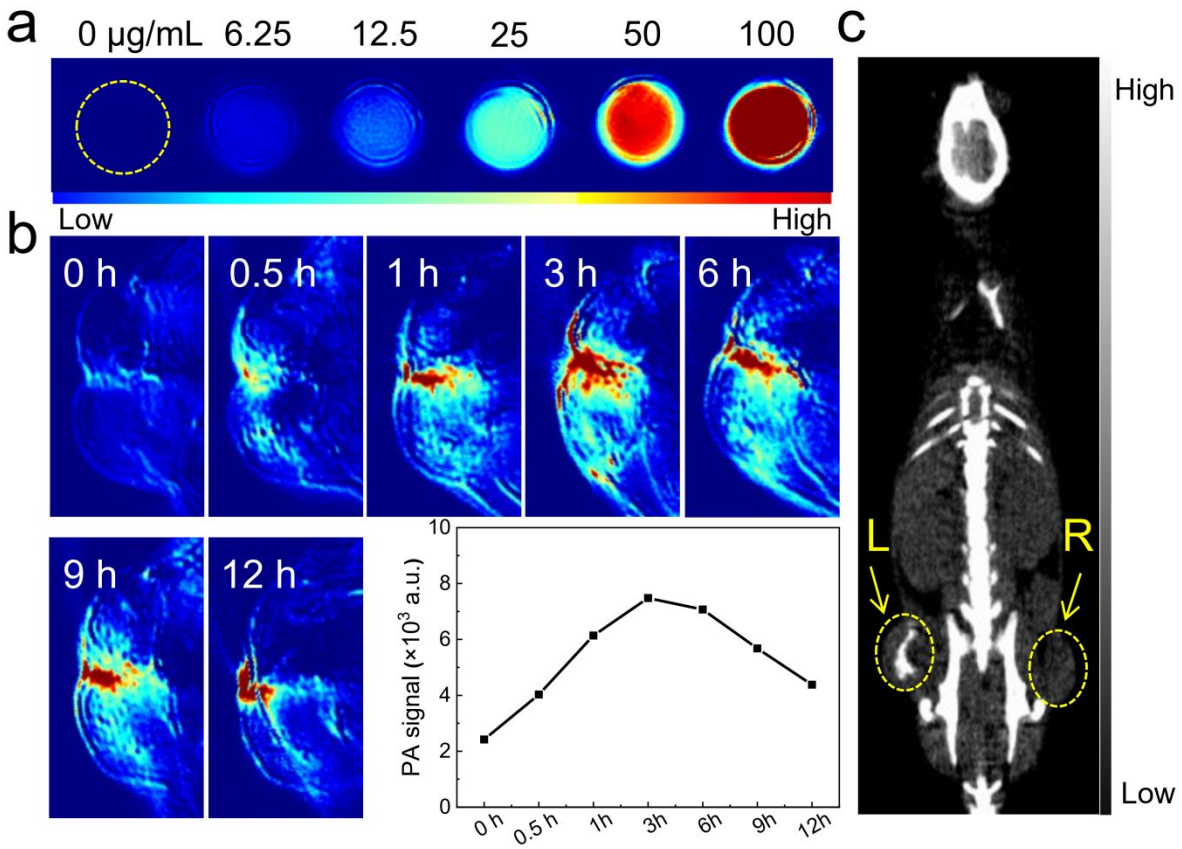

Figure 3. (a) PA images with different concentrations AuNBs@PDA nanocomplexes; (b) *in vivo* PA images of tumor bearing mice after intravenous injection with AuNBs@PDA nanocomplexes (2 mg/mL, 100 μL) acquired at different time points (inset: PA signal of tumor site); (c) CT images of the left and right tumor after intratumoral injection with AuNBs@PDA nanocomplexes and iopromide, respectively.

3.4 *In vivo* synergistic chemo-photothermal therapy

In light of the outstanding photothermal therapy effect on killing the tumor *in vitro*, next the infrared thermal imaging was used to study the photothermal effect of AuNBs@PDA nanocomplexes *in vivo*. As

shown in Figure 4a & 4b, the temperature of tumor site can be raised up 27.4 °C after AuNBs@PDA nanocomplexes injection under laser irradiation, but it was only raised up 12.5 °C upon the same laser irradiation in control tumor. To further show the synergistic chemo-photothermal therapy effect *in vivo*, tumor bearing BALB/c mice were stochasticly divided into four groups, which were laser only treatment (denoted as NIR), DOX plus laser treatment (denoted as DOX + NIR), AuNBs@PDA + NIR and AuNBs@PDA/DOX + NIR. The average tumor volumes of different treatments were represented for the therapeutic efficacy during 14 d of observation. As shown in Figure 4c & 4d, DOX + NIR treatment can slightly restrained the tumor growth as compared with the control laser treatment. While a moderate inhibition effect is appeared in the AuNBs@PDA + NIR group, indicating the efficient photothermal effect of AuNBs@PDA nanocomplexes in cancer therapy. By huge contrast, the tumor growth of AuNBs@PDA/DOX plus laser treatment was remarkably decreased in volume upon 808 nm irradiation. And the photos of tumors were also shown in Figure S8a post 14 d treatments. The antitumor efficacy was further evaluated using H&E staining of tumor tissues obtained on second post-treatment. As shown in Figure 4e, a large area of karyopyknosis and necrosis can be viewed in the tumor of AuNBs@PDA/DOX + NIR group compared with the other groups, which manifest the excellent synergistic chemo-photothermal efficacy of AuNBs@PDA/DOX nanocomplexes. In addition, the mice weight curves were obtained and displayed in Figure S8b. The weight of all four groups has negligible changed during the treatment observation period. And the major organs such as heart, liver, spleen, lung and kidney stained with H&E performed 14 days after treatments showed that there was no evident organ damage or inflammatory lesion in these major organs (Figure S9).

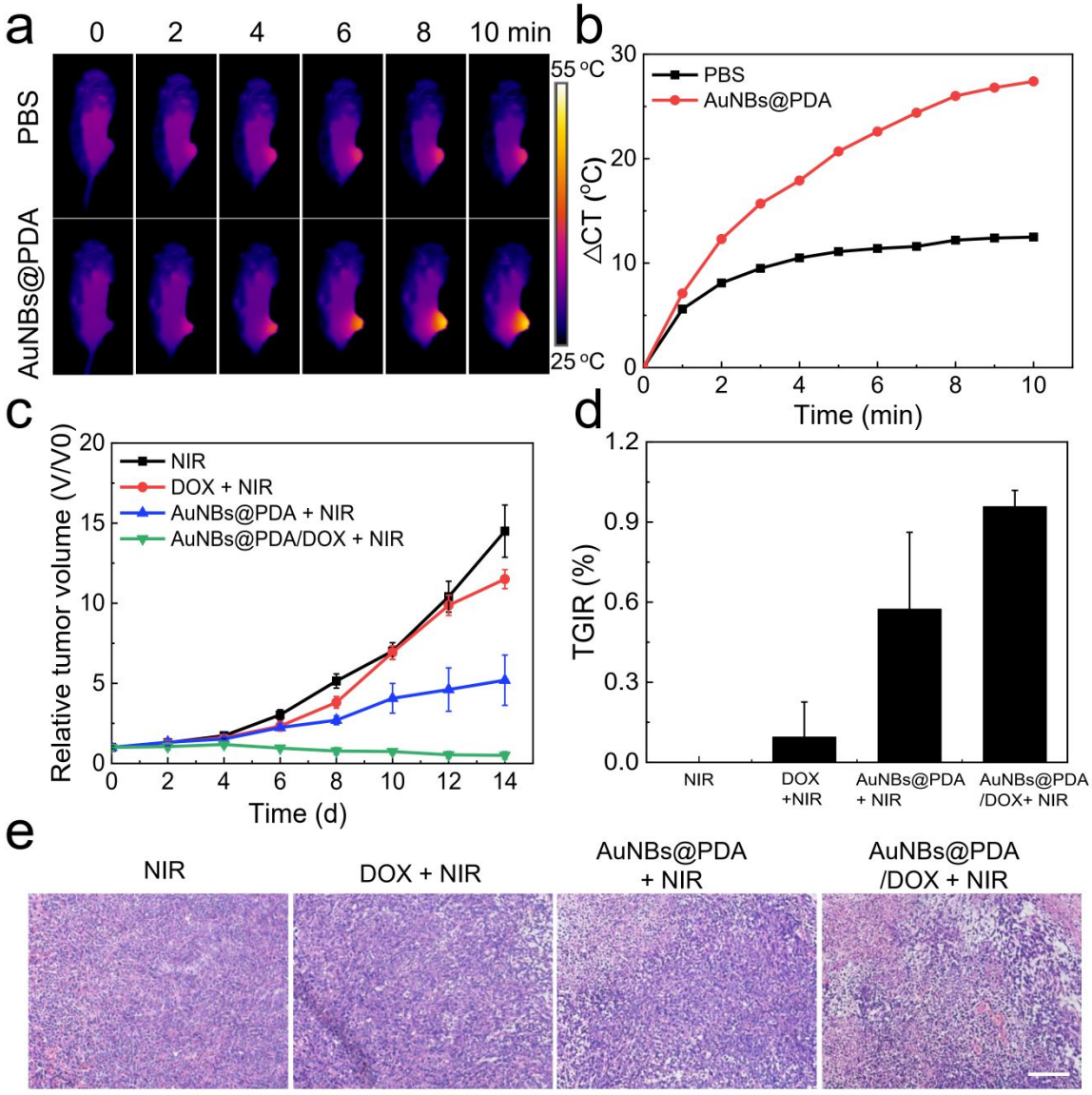

Figure 4. (a&b) Photothermal images and temperature changes of tumor-bearing mice under 808 nm laser irradiation (1 W/cm^2) after injection with PBS or AuNBs@PDA nanocomplexes (2 mg/mL, 100 μL); (c&d) Tumor volume growth curves and tumor growth inhibition ratio of mice after receiving different therapeutic treatments; (e) Slices of tumor tissues obtained and stained with H&E after receiving different therapeutic treatments, scale bar =100 μm.

4. Conclusions

In summary, we exploited a robust multifunctional nanoplatform for PA/CT imaging-guided chemo-photothermal therapy using AuNBs@PDA/DOX nanocomplexes. The AuNBs@PDA/DOX nanocomplexes as-synthesized have not only good dispersibility, biocompatibility and photo stability, but also high X-ray attenuation coefficient and strong NIR absorbance. These properties implied that AuNBs@PDA/DOX could form the basics of PA /CT imaging contrast and offered potential photothermal therapy clinical applications. Meanwhile, AuNBs@PDA/DOX could be triggered to release DOX by the lower pH environment and NIR laser irradiation. More excitingly, the results of *in vitro* and *in vivo* cancer therapy demonstrated that AuNBs@PDA/DOX nanocomplexes yielded outstanding chemo-photothermal therapy synergetic effect. Thus, we believe that the AuNBs@PDA/DOX nanocomplexes can be a novel multifunctional theranostic nanoagent for precision medicine.

Conflicts of interest

There are no conflicts to declare.

Acknowledgements

We acknowledge the financial support from National Key R&D program of China (2018YFB1105700),the National Natural Science Foundation of China (81902913, 81930048, 81627805), Guangdong Basic and Applied Basic Research Foundation for Distinguished Young Scholars (2020B1515020027), the Fundamental Research Funds for the Central Universities (19ykpy108), Natural Science Foundation of Jiangsu Province (BK20190821), the Postdoctoral Science Foundation of China (2019M651953), the Open Project Program of the State Key Laboratory of Radiation Medicine and Protection, Soochow University (GZK1201909), Guangdong Science and Technology Department (2017B030314026), the grants from Guangzhou Science and Technology Bureau, the Science and Technology Project from Suzhou City Commission of Health and Family Planning (LCZX201712), Opening Foundation of Hubei Province Key Laboratory of Molecular Imaging, and a Project Funded by the Priority Academic Program Development of Jiangsu Higher Education Institutions.

Notes and references

[1]. L. Cheng, C. Wang, L. Feng, K. Yang and Z. Liu, *Chem. Rev.* 114 (2014) 10869-10939.

[2]. S. Bertoni, Z. Liu, A. Correia, J. P. Martins, A. Rahikkala, F. Fontana, M. Kemell, D. Liu, B. Albertini, N. Passerini, W. Li and H. A. Santos, *Adv. Funct. Mater.* 28 (2018) 1806175.

[3]. M. P. Melancon, M. Zhou and C. Li, *Accounts Chem. Res.* 44 (2011) 947-956.

[4]. Y. Deng, X. Tian, S. Lu, M. Xie, H. Hu, R. Zhang, F. Lv, L. Cheng, H. Gu, Y. Zhao and Y. Pan, *ACS Appl. Mater. Interfaces* 10 (2018) 31106-31113.

[5]. Y. Deng, E. Li, X. Cheng, J. Zhu, S. Lu, C. Ge, H. Gu and Y. Pan, *Nanoscale* 8 (2016) 3895-3899.

[6]. R. Bardhan, S. Lal, A. Joshi and N. J. Halas, *Accounts Chem. Res.* 44 (2011) 936-946.

[7]. M. C. Chen, Z. W. Lin and M. H. Ling, *ACS Nano* 10 (2016) 93-101.

[8]. Y. Li, C. Jiang, D. Zhang, Y. Wang, X. Ren, K. Ai, X. Chen and L. Lu, *Acta Biomater.* 47 (2017) 124-134.

[9]. M. Zhang, L. Zhang, Y. Chen, L. Li, Z. Su and C. Wang, *Chem. Sci.* 8 (2017) 8067-8077.

[10]. S. Li, L. Zhang, X. Chen, T. Wang, Y. Zhao, L. Li and C. Wang, *ACS Appl. Mater. Interfaces* 10 (2018) 24137-24148.

[11]. Y. N. Xia, W. Y. Li, C. M. Cobley, J. G. Chen, X. H. Xia, Q. Zhang, M. X. Yang, E. Cho and P. K. Brown, *Accounts Chem. Res.* 44 (2011) 914-924.

[12]. H. H. Deng, L. N. Zhang, S. B. He, A. L. Liu, G. W. Li, X. H. Lin, X. H. Xia and W. Chen, *Biosens. Bioelectron* 65 (2015) 397-403.

[13]. Y. Tian, S. Qiang and L. Wang, *Front Bioeng. Biotechnol* 7 (2019) 398.

[14]. L. Zhang, M. Zhang, L. Zhou, Q. Han, X. Chen, S. Li, L. Li, Z. Su and C. Wang, *Biomaterials* 181 (2018) 113-125.

[15]. X. Cheng, X. Tian, A. Wu, J. Li, J. Tian, Y. Chong, Z. Chai, Y. Zhao, C. Chen and C. Ge, *ACS Appl. Mater. Interfaces* 7 (2015) 20568-20575.

[16]. L. Zhang, H. Su, J. Cai, D. Cheng, Y. Ma, J. Zhang, C. Zhou, S. Liu, H. Shi, Y. Zhang and C. Zhang,

ACS Nano 10 (2016) 10404-10417.

[17]. Y. Wang, Y. Liu, H. Luehmann, X. Xia, D. Wan, C. Cutler and Y. Xia, *Nano Lett.* 13 (2013) 581-585.

[18]. H. Bao, Y. Xia, C. Yu, X. Ning, X. Liu, H. Fu, Z. Chen, J. Huang and Z. Zhang, *Small* 15 (2019) e1904314.

[19]. W. Dong, Y. Li, D. Niu, Z. Ma, J. Gu, Y. Chen, W. Zhao, X. Liu, C. Liu and J. Shi, *Adv. Mater.* 23 (2011) 5392-5397.

[20]. H. Zhang, Q. Li, J. Huang, Y. Du and S. C. Ruan, *Sensors (Basel)* 16 (2016).

[21]. X. Yi, L. Chen, X. Zhong, R. Gao, Y. Qian, F. Wu, G. Song, Z. Chai, Z. Liu and K. Yang, *Nano Res.* 9 (2016) 3267-3278.

[22]. X. Ding, C. H. Liow, M. Zhang, R. Huang, C. Li, H. Shen, M. Liu, Y. Zou, N. Gao, Z. Zhang, Y. Li, Q. Wang, S. Li and J. Jiang, *J. Am. Chem. Soc.* 136 (2014) 15684-15693.

[23]. J. Wu, N. Kamaly, J. Shi, L. Zhao, Z. Xiao, G. Hollett, R. John, S. Ray, X. Xu, X. Zhang, P. W. Kantoff and O. C. Farokhzad, *Angew. Chem. Inter. Edi.* 53 (2014) 8975-8979.

[24]. J. Zhou, J. Li, X. Du and B. Xu, *Biomaterials* 129 (2017) 1-27.

[25]. D. C. S. Lio, C. Liu, M. M. S. Oo, C. Wiraja, M. H. Y. Teo, M. Zheng, S. W. T. Chew, X. Wang and C. Xu, *Nanoscale* 11 (2019) 17041-17051.

[26]. H. Lee, S. M. Dellatore, W. M. Miller and P. B. Messersmith, *Science* 318 (2007) 426-430.

[27]. Z. Li, Y. Hu, K. A. Howard, T. Jiang, X. Fan, Z. Miao, Y. Sun, F. Besenbacher and M. Yu, *ACS Nano* 10 (2016) 984-997.

[28]. C. K. Choi, J. Li, K. Wei, Y. J. Xu, L. W. Ho, M. Zhu, K. K. To, C. H. Choi and L. Bian, *J. Am. Chem. Soc.* 137 (2015) 7337-7346.

[29]. X. Liu, J. Cao, H. Li, J. Li, Q. Jin, K. Ren and J. Ji, *ACS Nano* 7 (2013) 9384-9395.

[30]. X. Wang, Z. Chen, P. Yang, J. Hu, Z. Wang and Y. Li, *Polym. Chem.* 10 (2019) 4194-4200.

[31]. Y. Zeng, D. Zhang, M. Wu, Y. Liu, X. Zhang, L. Li, Z. Li, X. Han, X. Wei and X. Liu, *ACS Appl.*

Mater. Interfaces 6 (2014) 14266-14277.

[32]. R. Zhang, S. Su, K. Hu, L. Shao, X. Deng, W. Sheng and Y. Wu, *Nanoscale* 7 (2015) 19722-19731.

[33]. C. Li, Z. Liu and P. Yao, *RSC Adv.* 6 (2016) 33083-33091.

[34]. G. Sun, T. Wang, X. Li, D. Li, Y. Peng, X. Wang, G. Jia, W. Su, C. Cheng, J. Yang and C. Zuo, *Adv. Healthc. Mater.* 7 (2018) e1800375.

[35]. S. Liu, L. Wang, M. Lin, D. Wang, Z. Song, S. Li, R. Ge, X. Zhang, Y. Liu, Z. Li, H. Sun, B. Yang and H. Zhang, *ACS Appl. Mater. Interfaces* 9 (2017) 44293-44306.

[36]. B. N. Khlebtsov, A. M. Burov, T. E. Pylaev and N. G. Khlebtsov, *Beilstein J. Nanotechnol.* 10 (2019) 794-803.

[37]. S. Wang, X. Zhao, S. Wang, J. Qian and S. He, *ACS Appl. Mater. Interfaces* 8 (2016) 24368-24384.

[38]. Y. H. You, Y. F. Lin, B. Nirosha, H. T. Chang and Y. F. Huang, *Nanotheranostics* 3 (2019) 266-283.

[39]. X. Zhao, T. Qi, C. Kong, M. Hao, Y. Wang, J. Li, B. Liu, Y. Gao and J. Jiang, *Int. J. Nanomedicine* 13 (2018) 6413-6428.

[40]. Z. Zhang, L. Wang, J. Wang, X. Jiang, X. Li, Z. Hu, Y. Ji, X. Wu and C. Chen, *Adv. Mater.* 24 (2012) 1418-1423.

[41]. Z. Zhang, J. Wang, X. Nie, T. Wen, Y. Ji, X. Wu, Y. Zhao and C. Chen, *J. Am. Chem. Soc.* 136 (2014) 7317-7326.

[42]. D. Zhang, M. Wu, Y. Zeng, L. Wu, Q. Wang, X. Han, X. Liu and J. Liu, *ACS Appl. Mater. Interfaces* 7 (2015) 8176-8187.

[43]. X. Zhong, K. Yang, Z. Dong, X. Yi, Y. Wang, C. Ge, Y. Zhao and Z. Liu, *Adv. Funct. Mater.* 25 (2015) 7327-7336.

[44]. N. Tahir, A. Madni, A. Correia, M. Rehman, V. Balasubramanian, M. M. Khan and H. A. Santos, *Int. J. Nanomedicine* 14 (2019) 4961-4974.

[45]. R. Xing, A. A. Bhirde, S. Wang, X. Sun, G. Liu, Y. Hou and X. Chen, *Nano Res.* 6 (2012) 1-9.

[46]. C. Wang, H. Xu, C. Liang, Y. Liu, Z. Li, Y. Guangbao, L. Cheng, Y. Li and Z. Liu, *ACS Nano* 7

(2013) 6782-6795.

[47]. Y. Jiang and K. Pu, *Small* 13 (2017).

[48]. X. Ning, H. Bao, X. Liu, H. Fu, W. Wang, J. Huang and Z. Zhang, *Nanoscale* 11 (2019) 20932-20941.

Fabrication of Multifunctional Polydopamine-Coated Gold Nanobones for PA/CT Imaging and Enhanced Synergistic Chemo-photothermal Therapy

Jingwei Xu,[a#] Xiaju Cheng,[b#] Fuxian Chen,[b] Weijie Li,[c] Xiaohui Xiao,[c] Puxiang Lai,[e] Guopeng Xu,[f] Li Xu,[f*] Yue Pan.[cd*]

[a] *Department of Cardiothoralic Surgery, Suzhou Municipal Hospital Institution, Suzhou, 215002, P.R. China.*

[b] *Jiangsu Key Laboratory of Infection and Immunity, Institutes of Biology and Medical Sciences, Soochow University, Suzhou 215123, P. R. China*

[c] *Guangdong Provincial Key Laboratory of Malignant Tumor Epigenetics and Gene Regulation, Medical Research Center, Sun Yat-Sen Memorial Hospital, Sun Yat-Sen University, Guangzhou 510120, P.R. China.*

[d] *Center for Precision Medicine, Sun Yat-Sen University, Guangzhou, 510080, P.R. China.*

[e] *The Hong Kong Polytechnic University, Department of Biomedical Engineering Kowloon, Hong Kong SAR, China.*

[f] *Department of Respiratory Medicine, Suzhou Municipal Hospital Institution, Suzhou, 215002, P.R. China.*

[#]*Equal contribution*

[*]*Corresponding author: xuli198008@126.com, panyue@mail.sysu.edu.cn*

Keywords: Imaging, Photothermal therapy, Multifunctional nanobones

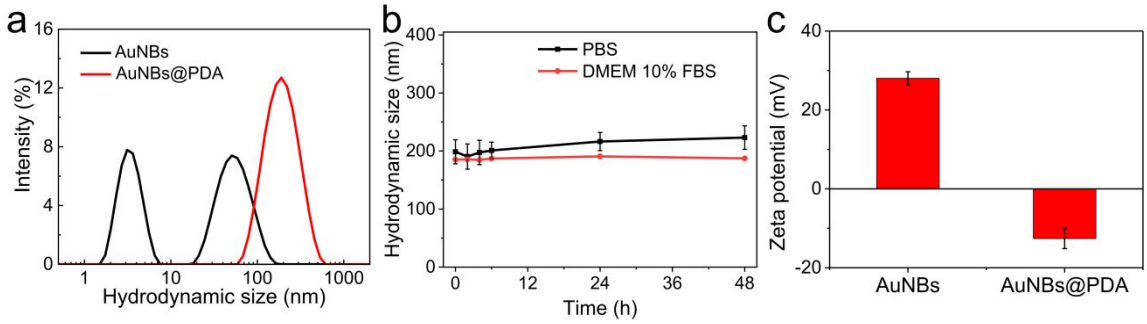

Figure S1. (a) Hydrodynamic size of AuNBs and AuNBs@PDA; (b) Hydrodynamic size of AuNBs@PDA nanocomplexes in PBS and 10% FBS DMEM medium monitored for 48 h. (c) Zeta potential of AuNBs and AuNBs@PDA.

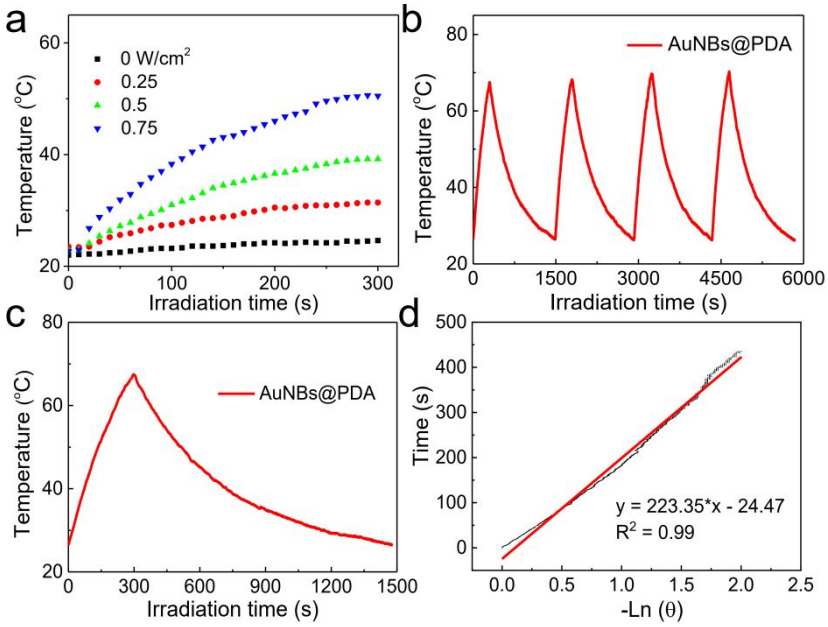

Figure S2. (a) The photothermal heating curves of AuNBs@PDA nanocomplexes (50 μg/mL) with different power density of 808 nm laser irradiation for 5 min; (b) Temperature elevation of AuNBs@PDA nanocomplexes (100 μg/mL) over four laser on/off cycles; (c) The monitored temperature profile over 1500 s of a AuNBs@PDA nanocomplexes aqueous solution (100 μg/mL) irradiated by laser for 300 s, followed by natural cooling with laser light turned off; (d) Plot of cooling time versus negative natural logarithm of the temperature difference, obtained from the cooling stage. The time constant for heat transfer of the system is determined to be τs = 223.35 s.

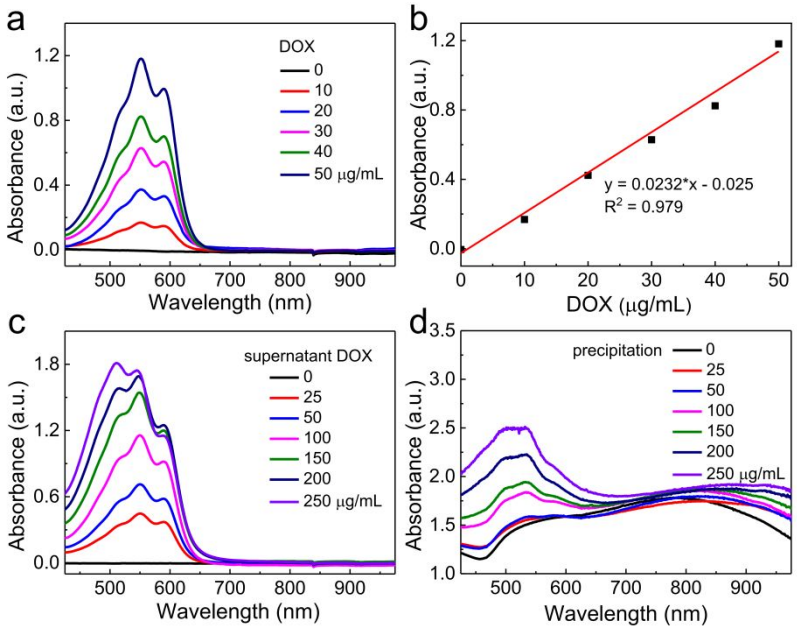

Figure S3: (a&b) Vis-NIR absorbance spectra of free DOX obtained at different concentrations; (c&d) Vis-NIR absorbance spectra of supernatant DOX and precipitation AuNBs@PDA/DOX obtained at different DOX feeding.

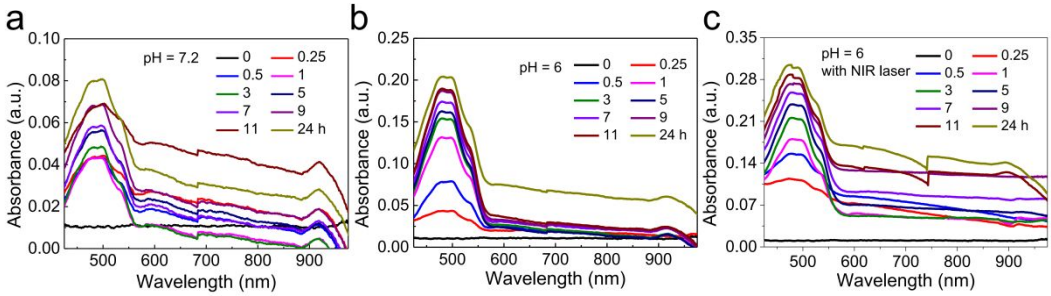

Figure S4: (a&b) Vis–NIR absorbance spectra of DOX released from AuNBs@PDA/DOX nanocomplexes in different pH values (7.2 and 6) buffers and DOX release from AuNBs@PDA/DOX nanocomplexes at pH values of 6 with NIR laser irradiation.

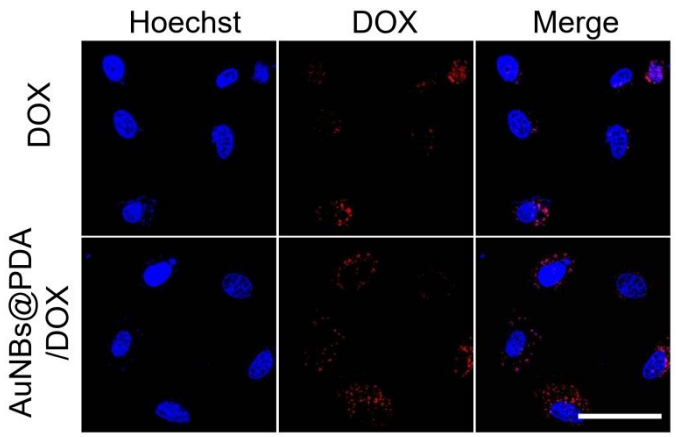

Figure S5. Cellular uptake of free DOX and AuNBs@PDA/DOX nanocomplexes. Scale bar = 30 μm.

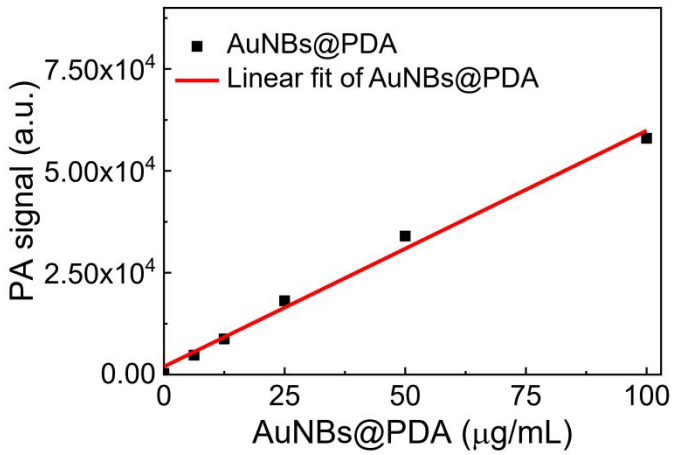

Figure S6. PA signal of different concentrations AuNBs@PDA nanocomplexes.

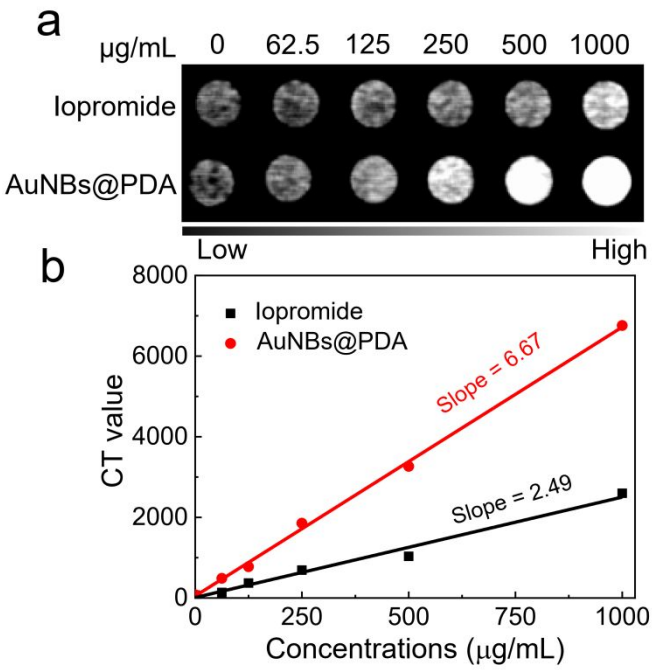

Figure S7. (a&b) CT images and CT value (HU) of different concentrations AuNBs@PDA nanocomplexes and iopromide.

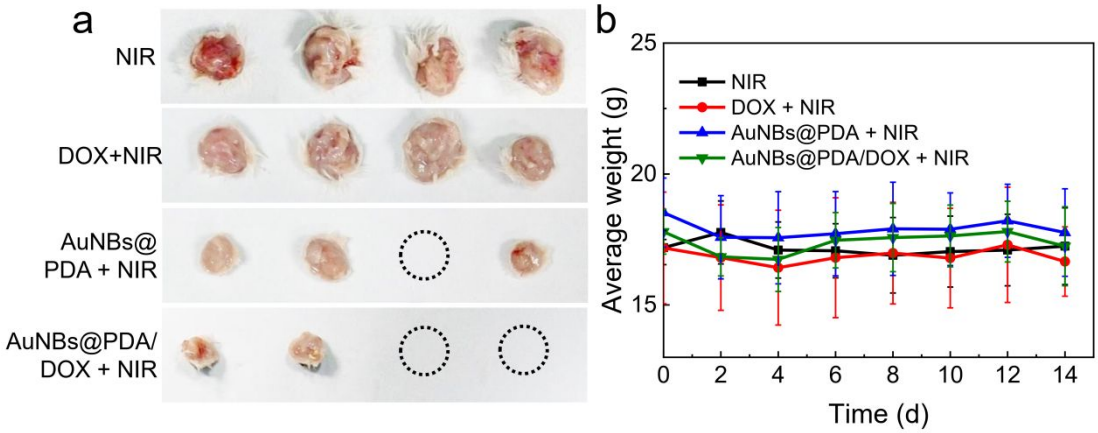

Figure S8. (a&b) Photos of tumors and average body weight of mice post 14 days treatments.